COMPARISON OF HELICOPTER-BORNE MEASUREMENTS OF SEA ICE THICKNESS AND SURFACE ROUGHNESS WITH SAR SIGNATURES

Thomas Busche[(1)], Carola von Saldern[(1)], Christian Haas[(1)], Wolfgang Dierking[(1)]

[(1)]Alfred Wegener Institute for Polar and Marine Research, Bussestr. 24, D-27570 Bremerhaven, Germany, Email:
tbusche@awi-bremerhaven.de
csaldern@awi-bremerhaven.de
chaas@awi-bremerhaven.de
wdierking@awi-bremerhaven.de

ABSTRACT

Although sea ice thickness is not directly measured by means of radar sensors, its magnitude and variations are to a certain degree reflected by the sea ice surface characteristics. Establishing simple but robust empirical relationships between sea ice surface properties and SAR signatures is an alternative to a much more complex theoretical microwave modelling approach for sea ice mapping.

In this study correlations between helicopter-borne sea ice thickness and roughness measurements and SAR signatures are investigated. Preliminary results from a comparison of a Radarsat-1 scene and sea ice thickness data are presented. The profiles and histograms show a good agreement between SAR backscatter and sea ice thickness, while the correlation coefficient of $R^2 = 0.2$ indicates a very poor relationship. One source of error considered as the reason for the poor correlation is a remaining co-registration error due to insufficient ice drift data and the immanent sensor accuracies. But as the main source of ambiguity the variety of different scattering mechanisms typical for multiyear ice is discussed. Further analysis of the thickness and the laser roughness data in conjunction with the SAR profiles is planned to identify roughness parameters that are connected to the backscattering behaviour of multiyear sea ice surfaces and indirectly to its thickness.

1. INTRODUCTION

Deriving sea ice thickness information by means of imaging SAR sensors is one of the most desired but still most challenging tasks. Several case studies have been carried out in the last decades and are reported in the literature. Two different approaches can be categorized for simplification to retrieve ice thickness information from SAR measurements:
A more indirect approach is presented in [1] by establishing a classification scheme for SAR imagery which uses dynamic local thresholding as a classification basis and then supplements that initial classification using heuristic geophysical knowledge organized in expert systems, resulting in different thickness classes.

Other studies propose more direct but empirical techniques to quantify sea ice thickness from SAR measurements. Reference [2] presents a simple linear modelling technique which relates ridge frequency extracted from SAR images to keel draft from sonar with high correlation.
A case study for Arctic sea ice in [3] establishes in a direct comparison a linear relationships between mean SAR backscatter measured by an airborne X-band SAR sensor and mean ice draft measured by sonar and also mean elevation from laser profiling; the resulting best correlation coefficients are determined for laser data with $R^2 = 0.51$ and slightly better for sonar draft data with $R^2 = 0.68$. In a similar fashion [4] reports for a study area in the Sea of Okhotsk a correlation coefficient between calibrated L-Band HV backscatter from a high resolution airborne sensor and draft data with $R^2 = 0.64$. The main disadvantage of these encouraging findings is that the resulting empirical models cannot be used for SAR scenes with different sensor constellation or those that are separated in space or time.
Other method to retrieve sea ice thickness partly based on theoretical models are summarized in [5] using polarimetric SAR data from JPL's AIRSAR-system, but the latter is limited to the retrieval of young and very thin sea ice thicknesses.
Besides the development of advanced algorithms, that are subject of ongoing work at AWI, the data available for this study gives the opportunity to check some of the cited simple empirical methods. The preliminary results shown here are oriented on [3] and [4], and are a direct comparison of SAR backscatter with helicopter-borne measurements of sea ice thickness.

Proc. of the 2004 Envisat & ERS Symposium, Salzburg, Austria 6-10 September 2004 (ESA SP-572, April 2005)

2. DATA AND STUDY AREA

The data studied here have been collected during the CryoVex2003 campaign that took place in the European Arctic in the Barents Sea and Fram Strait area from February 28 to April 24 2003 as part of the winter cruise ARK 19/1 of AWI's icebreaker and research vessel Polarstern. CryoVex2003 was the first pre-launch validation experiment for the CryoSat mission within the framework of the Sea Ice Thickness Observing Project (SITHOS), whose overall objective is to develop a European monitoring systems for sea ice thickness and related parameters. Besides ground based methods like ice coring and snow sampling several airborne techniques were evaluated during the campaign including laser profiling and scanning combined with cinematic GPS, radar altimetry and electromagnetic induction sounding combined with laser altimetry. Coincident to ground sampling and measurement flights a collection of SAR imagery was acquired from the sensors of Envisat, Radarsat-1 and ERS-2. The preliminary results presented here are obtained from a Radarsat-1 scene with HH polarization from a descending orbit from April 11 2003 and a measurement flight of the helicopter-borne EM-Bird, AWI's electromagnetic sounding device

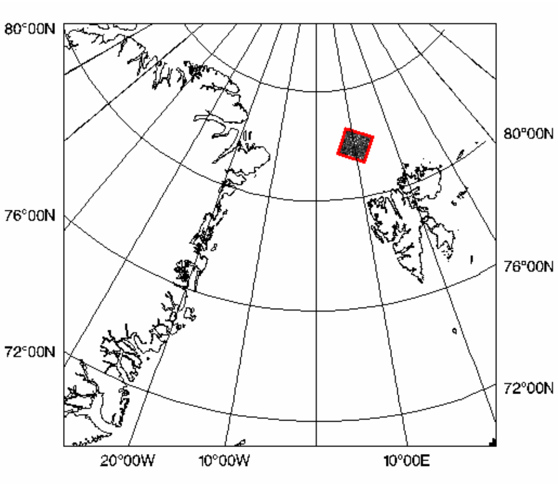

Fig. 1. The study area with Radarsat-1 scene

The EM-Bird consists of two sensors. A laser altimeter measures the distance between the sensor and the sea ice surface and an electromagnetic device measures the distance between the sensor and the sea ice-seawater interface The difference between both distances is the resulting sea ice thickness. The laser data is processed separately by eliminating platform motions from the data to a pseudo freeboard that is related more to local minima than to the geoids surface, see [6] for details. A typical sensor height of 15m above ground and platform speed of 30-40 m/s in conjunction with different sampling frequencies of both sensors gives a spatial sampling interval on the ground of around 2m for the ice thickness and 0.3m to 0.4m for the laser data.

The location of the Radarsat-1 scene is shown in Fig. 1. The processing of the SAR scene and the sea ice thickness data consisted of the following steps:

1. Speckle suppression by adaptive filtering using a gamma map filter within a 11x11 pixel window
2. Absolute calibration, calculating σ^0 values
3. Geocoding to a UTM projection
4. Co-registration of the EM-Bird flight profile, with a length of 17.5km, correcting for ice drift due to temporal differences in SAR and EM-Bird data acquisition. This was done using GPS ship positions from Polarstern. At the date of image acquisition the vessel was rammed into a floe drifting free within the ice pack. The resulting ice drift expressed in a time difference of 5h was calculated to an offset of 380m in Northing and 448m in Easting direction.
5. Extracting SAR backscatter along the flight track using a 5 x 5 pixel window averaging the sea ice thickness.

3. RESULTS AND DISCUSSION

Fig. 2 shows a zoom in the Radarsat-1 scene from April 11 2003 overlaid with the EM-Bird flight track not corrected for ice drift, with the sea ice thickness colour-coded from red i.e. very thick to dark blue i.e. thin thicknesses. The resulting ice drift vector is marked with a red arrow. The scene is dominated by large multiyear flows (medium to light grey) embedded in a matrix of young and first year ice (very dark to dark grey). The filtering accentuates light features on the multiyear floes that can be interpreted, if surrounded by a zone of higher grey value variability, as zones of deformed ice. Even single ridges can be identified, while the smooth level ice shows low grey value variability.

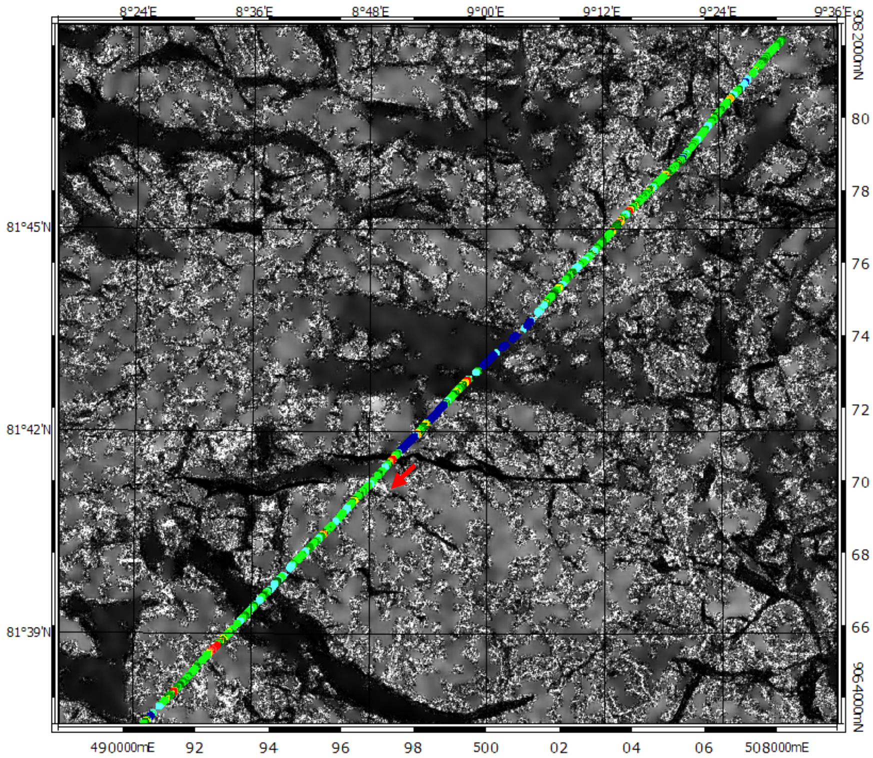

Fig. 4. Zoom into the Radarsat-1 scene from April 11, 2003. The line is the EM-Bird flight track with the sea ice thickness colour-coded, the red arrow marks the resulting ice drift vector

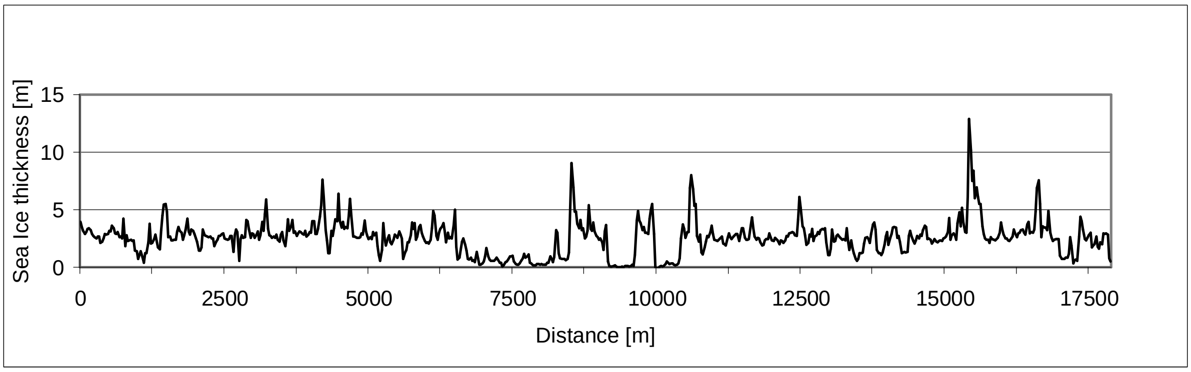

Fig.3a. EM-bird profile of sea ice thickness

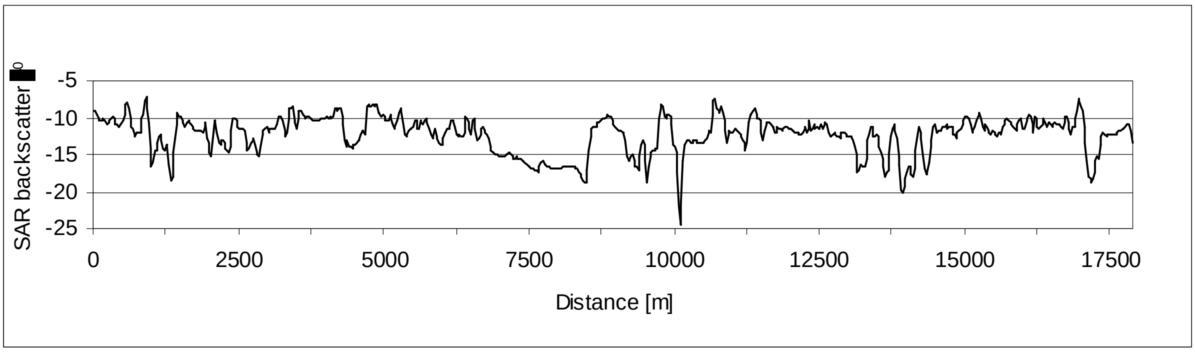

Fig 3b. Radarsat-1 SAR backscatter profile

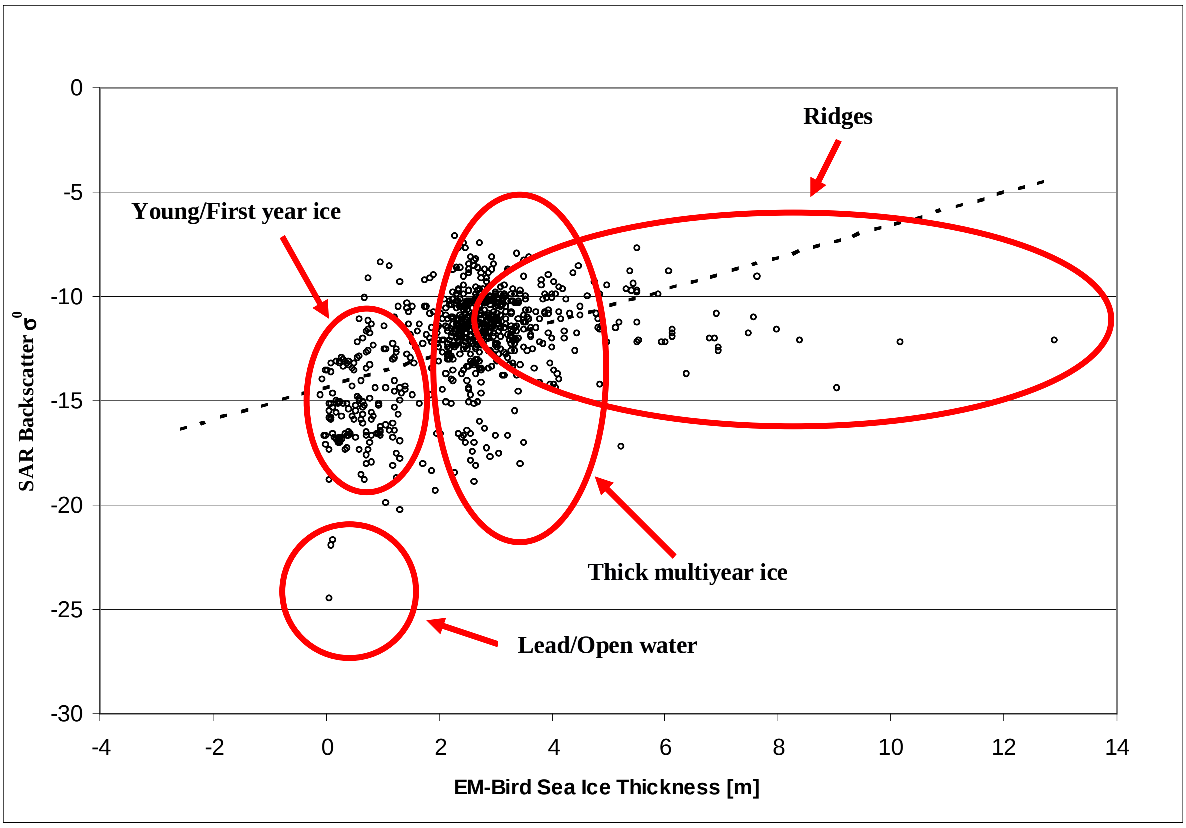

Fig. 4. Scatterplot of EM-Bird sea ice thickness vs. SAR backscatter σ^0, n = 716, R^2 = 0.2039

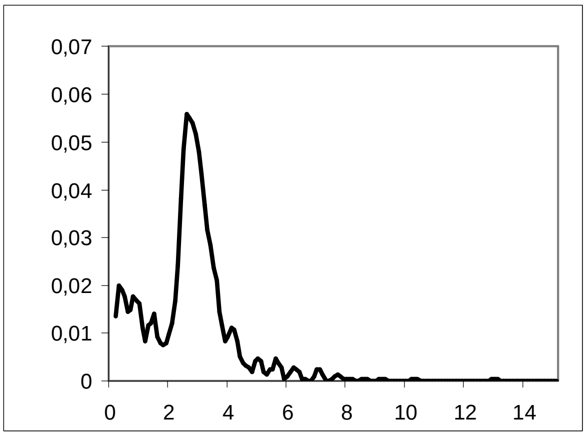

Fig. 5a Histogram EM-Bird sea ice thickness

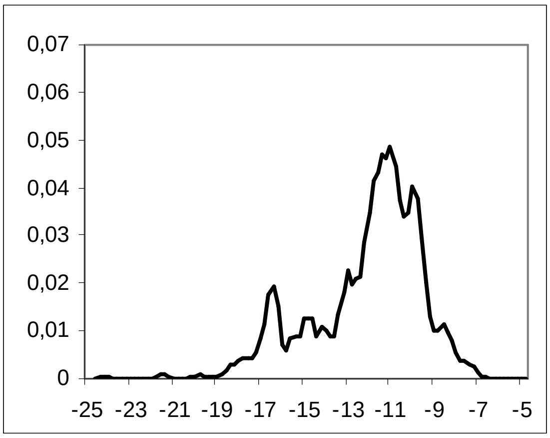

Fig. 5b. Histogram SAR backscatter σ^0

Fig. 3a shows the profile of the sea ice thickness measured by the EM-Bird, Fig. 3b. the corresponding backscattering coefficient along the flight path. The SAR profile is in moderate to good agreement with the thickness profile, with some exceptions. At around 10100m profile length a remarkable drop in the backscattering profile near to the noise floor can be observed, the drop in the thickness profile is less pronounced. It is assumed that this is an open lead likely refrozen and covered with very thin ice. There is also a high peak in the thickness profile at around 15400m with a extreme value of thickness of the order of 12m which has no correspondence in the backscattering profile. This could be either due to a remaining mismatch in the co-registration or due to a keel without a associated or less accentuated or weathered sail at the ice surface. And last but not least this could be a ridge oriented parallel to the radar beam, highlighting another source of ambiguity of such a direct comparison.

Fig. 4 shows a scatter plot for all data points of the profile, thickness vs. backscattering coefficient. The correlation is very poor, with a correlation coefficient R^2 = 0.2, what is far away from the good relationship reported in [4] for L-band SAR in an environment of young and first year ice and also in [3] for a X-band SAR in Artic multiyear ice. On the other hand is the scatter plot visually very similar to the one shown in [4]. The point clouds in Fig. 4. are highlighted and interpreted here as ice classes. It is obvious that pressure ridges or zones of high thickness cannot be very well separated by their backscattering coefficient from level multiyear ice. The latter has backscattering signatures covering nearly the whole range of the spectrum, reflecting, on the one hand, the different scattering mechanisms involved in the radar backscattering from multiyear ice. On the other hand has a small mismatch in the co-registration procedure for the ridges with an extent in the image of normally 1 to 2 pixels the consequences of an underestimation of the backscatter signal, especially for ridges marking the edge of a floe next to thin young ice or a refrozen lead.

It is expected that an averaging along the flight track with larger window sizes will improve the correlation as it was observed in [3]. Incidence angle effects can be neglected due to the relatively short length of the profile and the small range of incidence angles from 35.63 to 41.72 degree.

The histograms of both profiles shown in Fig. 5a and Fig. 5b look similar as observed for the profiles. According to the scatter plot in Fig. 4 the different ice classes can be identified, where the lower tail in both histograms marks the young and first year ice and the upper tail, with an apparent different slope, can be interpreted as ridges. The middle part around the mean value represents the thick multiyear ice, with a mean value of 2.5m for the thickness and –12.38dB for the SAR backscatter. Here it is also obvious that a close range of thickness has not a direct counterpart in the backscatter histogram. These indicates that a retrieval of sea ice thickness, using simple linear models that are based on mean SAR backscatter values alone, is not feasible because of the dependence of the backscattering to more than one scattering mechanism.

4. CONCLUSION AND OUTLOOK

It has been observed that a direct comparison of sea ice thickness with SAR backscatter gives quite poor results expressed in a very low value of the correlation coefficient. One possible explanation is the remaining uncertainty in the co-registration procedure induced by insufficient ice drift data and also to the sensor immanent inaccuracies. For future missions a set of buoys in the vicinity of the sampling area would help to reconstruct the drift situation, a set of ground control points marked by transponders and placed on the ice is an alternative. A time series of SAR scenes would also help to correct for ice drift. The usage of larger window sizes for extracting the data along track will also improve the results of the correlation.

It is assumed that the main reason for the bad correlation is the variability of the scattering mechanisms. It is still unclear if multiple scattering effects or volume scattering causes this wide range of backscatter values for the level multiyear ice. Further analysis of the thickness and the laser roughness data in conjunction with the SAR profiles is required. If multiple scattering caused by higher roughness in deformed ice zones is the main reason for this phenomenon then the horizontal and vertical spatial resolution of the laser sensor could be sufficient to identify statistical parameters that are connected to the backscattering behaviour of multiyear sea ice surfaces and indirectly to its thickness. A combination of methods also considering the ridge statistics with respect to the thickness distribution as proposed by [2] is imaginable and will be investigated in future work.

5. REFERENCES

1. Haverkamp, D., Soh, L. K., Tsatsoulis, C. A Comprehensive, Automated Approach to Determining Sea Ice Thickness from SAR Data.. *IEEE Trans. Geosc Remote Sensing*, Vol. 33, No. 1, 46 – 57, 1995.

2. Melling, H. Detection of features in first-year pack ice by synthetic aperture radar (SAR). *Int. J. Remote Sensing*, Vol. 19, No. 6, 1223 – 1249, 1998

3. Comiso, J.C., Wadhams, P., Krabill, W. B., Swift, R. N., Crawford, J. P., Tucker III, B. Top/Bottom Multisensor Remote Sensing of Artic Sea Ice. *J. Geophysical Research*, Vol. 96, No. C2, 2693 – 2709, 1991

4. Matsuoko, T., Uratsuka, S, Satake, M., Nadai, A., Umehara, T., Maeno, H., Wakabayashi, H., Nishio, F., Fukumachi, Y. Deriving sea-ice thickness and ice-types in the Sea of Okhotsk using dual-frequency airborne SAR (Pi-SAR) data. *Annals of Glaciology*, Vol. 34, 429 – 434, 2002.

5. Kwok, R., Nghiem, S. V., Martin, S., Winebrenner, D. P., Gow, A. J., Perovich, C.T., Swift, C.T., Barber, D.G., Golden, K. M., Knapp, E. J., Laboratory Measurements Of Sea Ice: Connection to Microwave Remote Sensing. *IEEE Trans. Geosc. Remote Sensing*, Vol. 36, No. 5, 1716 – 1730, 1998.

6. Dierking, W. Laser profiling of the ice surface topography during the winter Weddell Gyre Study 1992. *J. Geophysical Research*, Vol. 100, No. C3, 4807 – 4820, 1995.